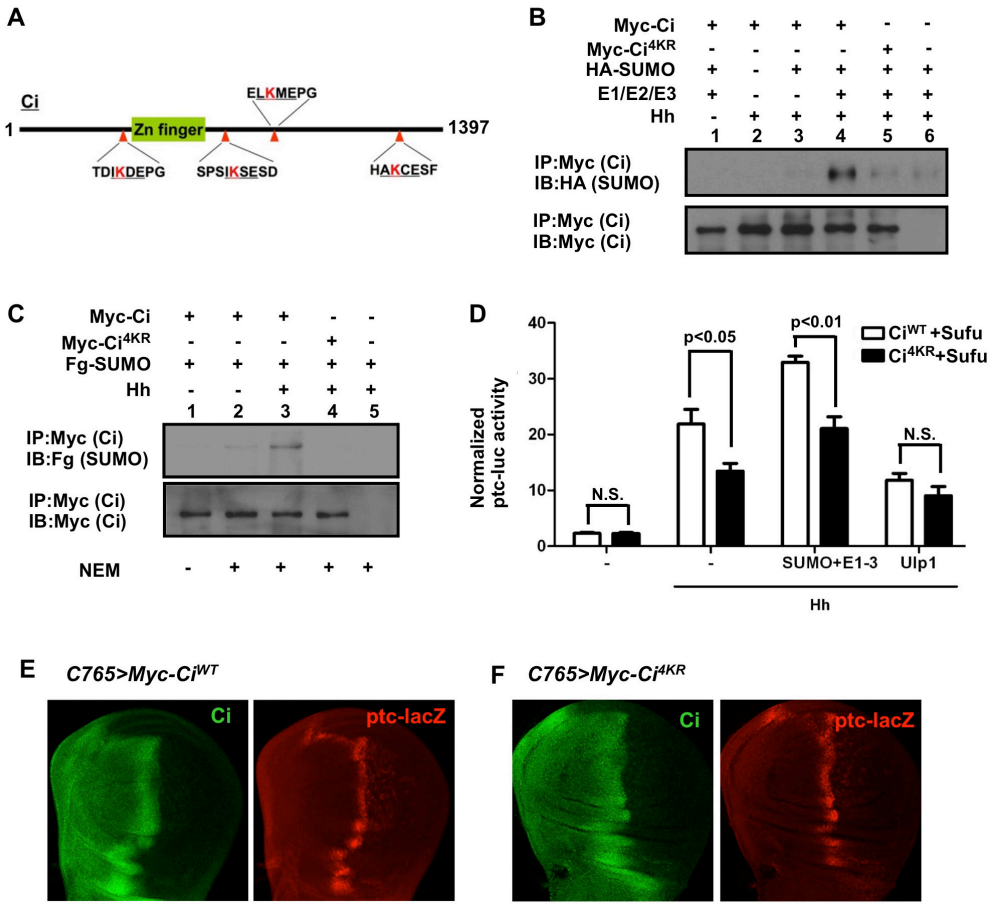

Figure S1 Hh stimulates sumoylation of Ci–related to Figure 1

(A) Schematic drawing of Ci with the Zn-finger DNA binding domain indicated by a green bar and the SUMO acceptor sites indicated by red triangles. (B-C) Western blots to detect SUMO-conjugated Ci derived from S2 cells transfected with the indicated constructs and treated with or without Hh-conditioned medium. NEM was added to the cell lysates to preserve SUMO conjugated Ci (C). Hh stimulates sumoylation of Myc-Ci but not Myc-Ci^{4KR} in which the four Lys residues in the SUMO acceptor consensus sites were converted to Arg. (D) *ptc-luc* assay in S2 cells transfected with the indicated constructs and treated with or without Hh-conditioned medium. Data are means ± SEM of normalized *ptc-luc* activity from three independent experiments. (E-F) Late third instar larval wing discs expressing Myc-Ci or Myc-Ci^{4KR} under the control of *C765* were immunostained for Ci (green) and *ptc-lacZ* (red) expression.

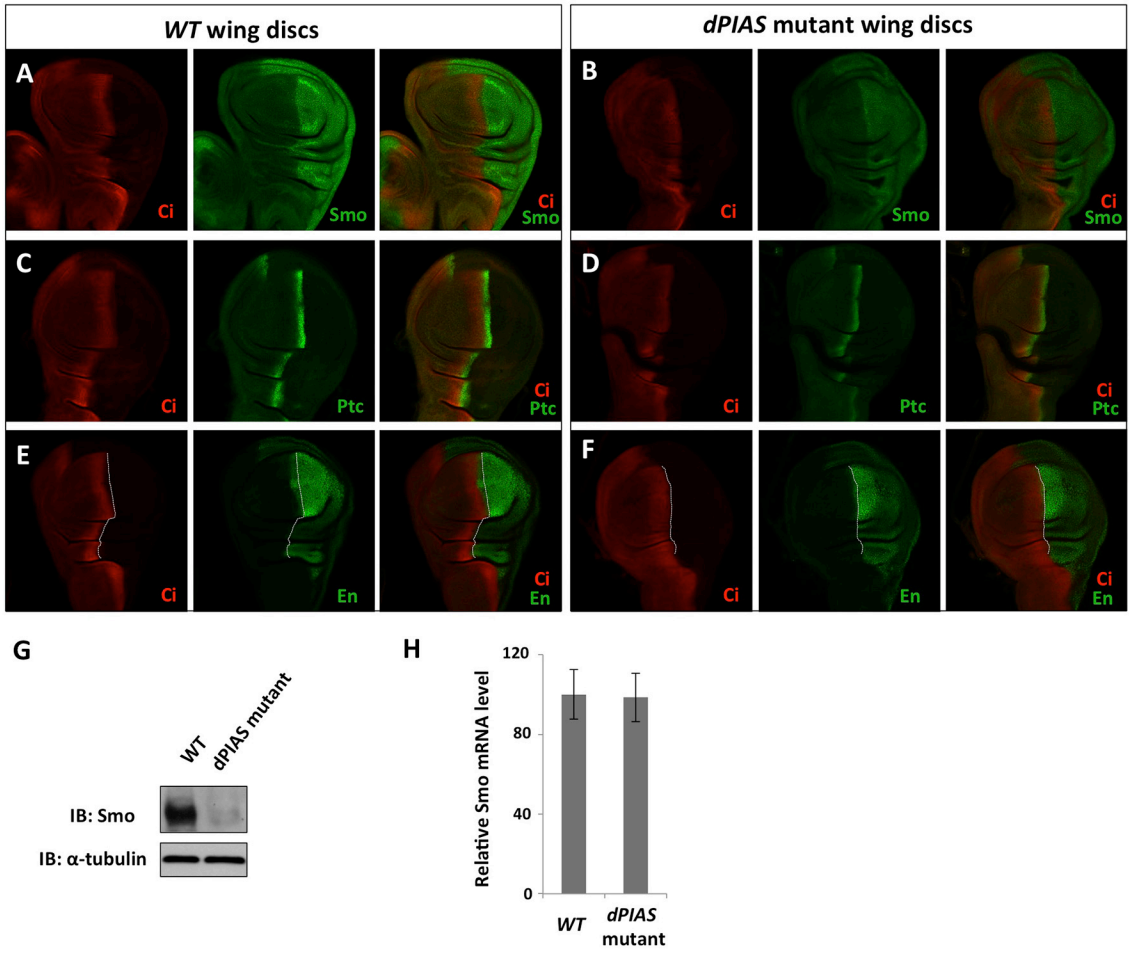

Figure S2 dPIAS mutant wing discs exhibited reduced Smo level and Hh pathway activity- related to Figure 2

(A-F) Wing discs from late third instar wild type (A, C, E) or *dPIAS* transheterozygous *Su(var)2-10*^{03697}*/Su(var)2-10*^{2} (B, D, F) larvae were immunostained to show the expression of Ci (red) and Smo, Ptc, or En (green). Dashed lines demarcate the A/P boundary (E0F). *dPIAS* transheterozygous larvae were recognized by the presence of melanotic tumors. *dPIAS* mutant discs exhibited reduced accumulation of Smo as well as reduced expression of Ptc and En expression in A compartment cells near the A/P boundary. (G-H) Western blot (G) and qRT-PCR (H) to show Smo protein expression or mRNA level in wild type and *dPIAS* transheterozygous mutant wing discs, respectively. Proximally 30 wing discs for each genotype were used for western blot analysis.

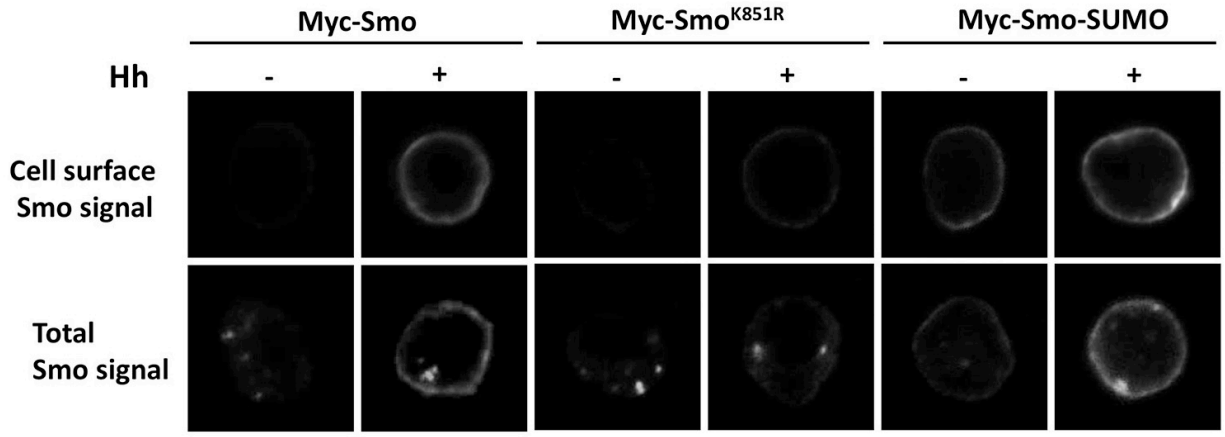

Figure S3 Sumoylation of Smo regulates its cell surface expression–related to Figure 3

S2 cells transfected with the indicated Myc-Smo constructs and treated with or without Hh-conditioned medium were immunostained with anti-SmoN antibody before membrane permeabilization to visualize cell surface Smo signals or with anti-Myc antibody after membrane permeabilization to examine the total Smo signals. The sumoylation deficient Smo (Myc-Smo^{K851R}) exhibited diminished cell surface accumulation in response to Hh stimulation whereas the sumo-mimetic form (Smo-SUMO) exhibited high basal cell surface expression.

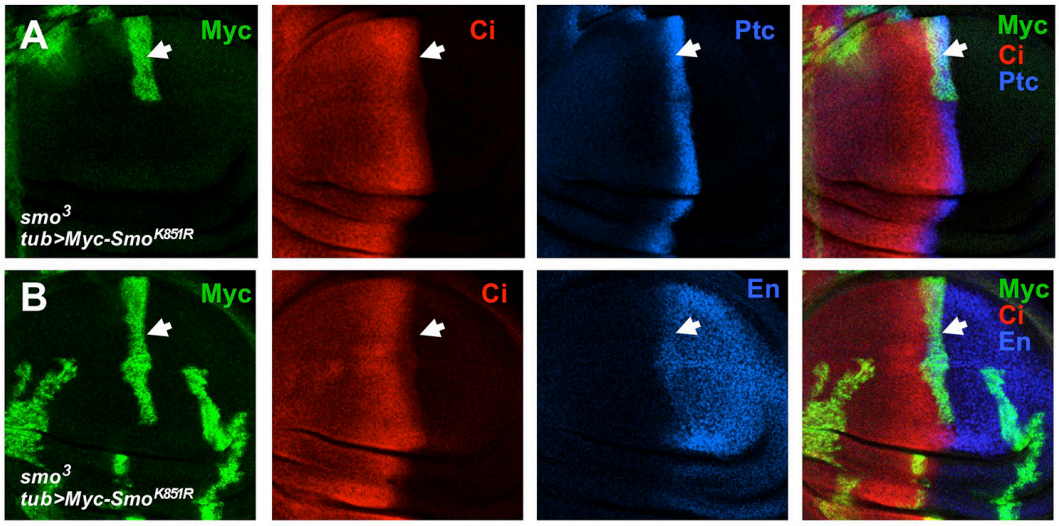

Figure S4 Overexpression of Smo^{K851R} rescues *smo* phenotype–related to Figure 4

(A-B) Late third instar larval wing discs containing *smo*^{3} clones that express Myc-Smo^{K851R} under the control of *tub-Gal4* were immunostained to show the expression of Myc (green), Ci (red), and Ptc or En (blue). *smo* mutant clones expressing the *smo* transgene are marked by Myc staining. Arrowheads indicate clones near the A/P boundary. Overexpression of Myc-Smo^{K851R} in *smo* mutant clones restored the expression of both *ptc* and *en*.

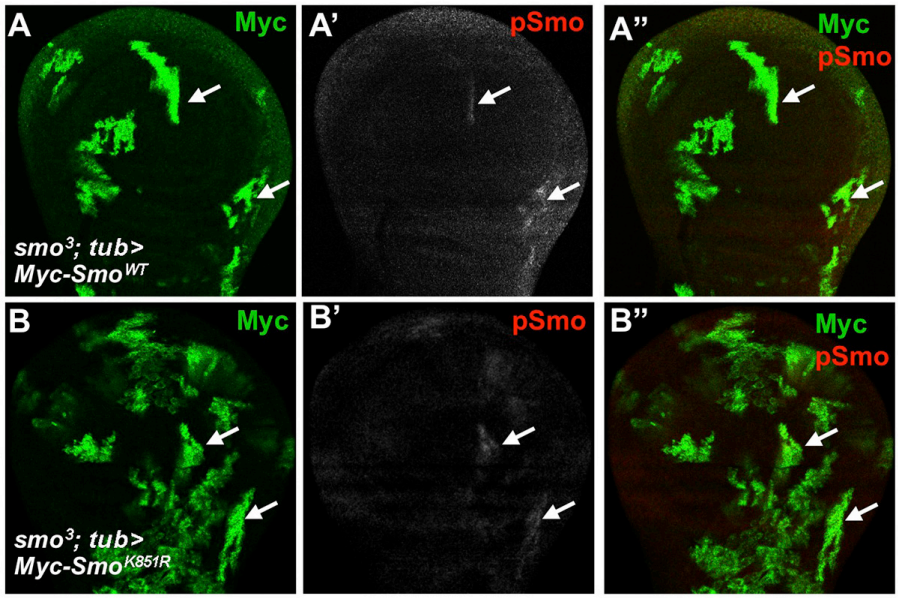

Figure S5 Blocking Smo sumoylation does not affect its phosphorylation–related to Figure 5

(A-B") Late third instar larval wing discs containing *smo*^{3} clones that express either wild type Myc-Smo (A-A") or Myc-Smo^{K851R} (B-B") under the control *of tub-Gal4* were immunostained with Myc antibody and a phospho-specific antibody (pSmo) that recognizes phosphorylated S687, S690, and S693 on Smo. Myc-Smo and Myc-Smo^{K851R} -expressing clones in the P-compartment or near the A/P boundary but not in the A-compartment away from the A/P boundary exhibited pSmo signals (arrows).

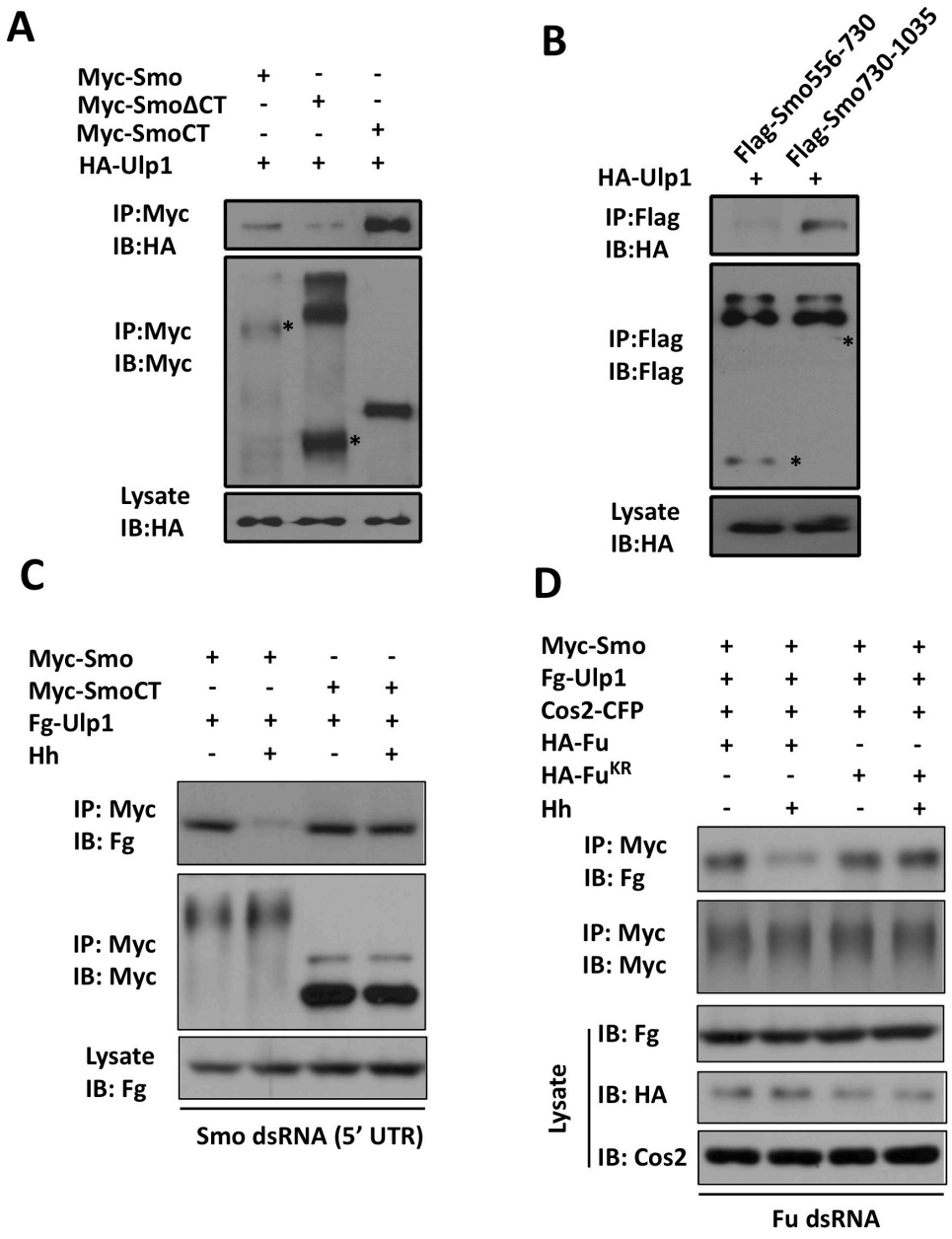

Figure S6 Ulp1 binds to the C-terminal region of Smo C-tail–related to Figure 5

(A-C) Cell lysates derived from S2 cells transfected with the indicated Smo constructs and HA-Ulp1 and treated with or without Hh conditioned medium were immunoprecipitated with Myc or Flag antibody, followed by western blot analysis with the indicated antibodies. Cell lysates were also directly subjected to western blot analysis with the HA antibody. Asterisks indicate the monomeric full-length and truncated Smo. Ulp1 binds strongly to the C-terminal half of Smo C-tail (Smo730-1035). Of note, endogenous Smo was knocked down by dsRNA targeting its 5'

UTR (C). SmoCT/Ulp1 interaction was no longer downregulated by Hh. (D) Fu kinase activity is required for Hh-mediated downregulation of Smo/Ulp1 interaction. Cell lysates derived from S2 cells transfected with the indicated constructs and treated with or without Hh conditioned medium were immunoprecipitated with Myc, followed by immunoblotting with, or directly blotted with the indicated antibodies. Of note, RNAi-resistant wild type (HA-Fu) or kinase dead Fu (HA-Fu^{KR}) construct was transfected to replace endogenous Fu, which was depleted by RNAi (see method for detail). HA-Fu but not HA-Fu^{KR} mediated the inhibition of SmoCT/Ulp1 interaction by Hh.

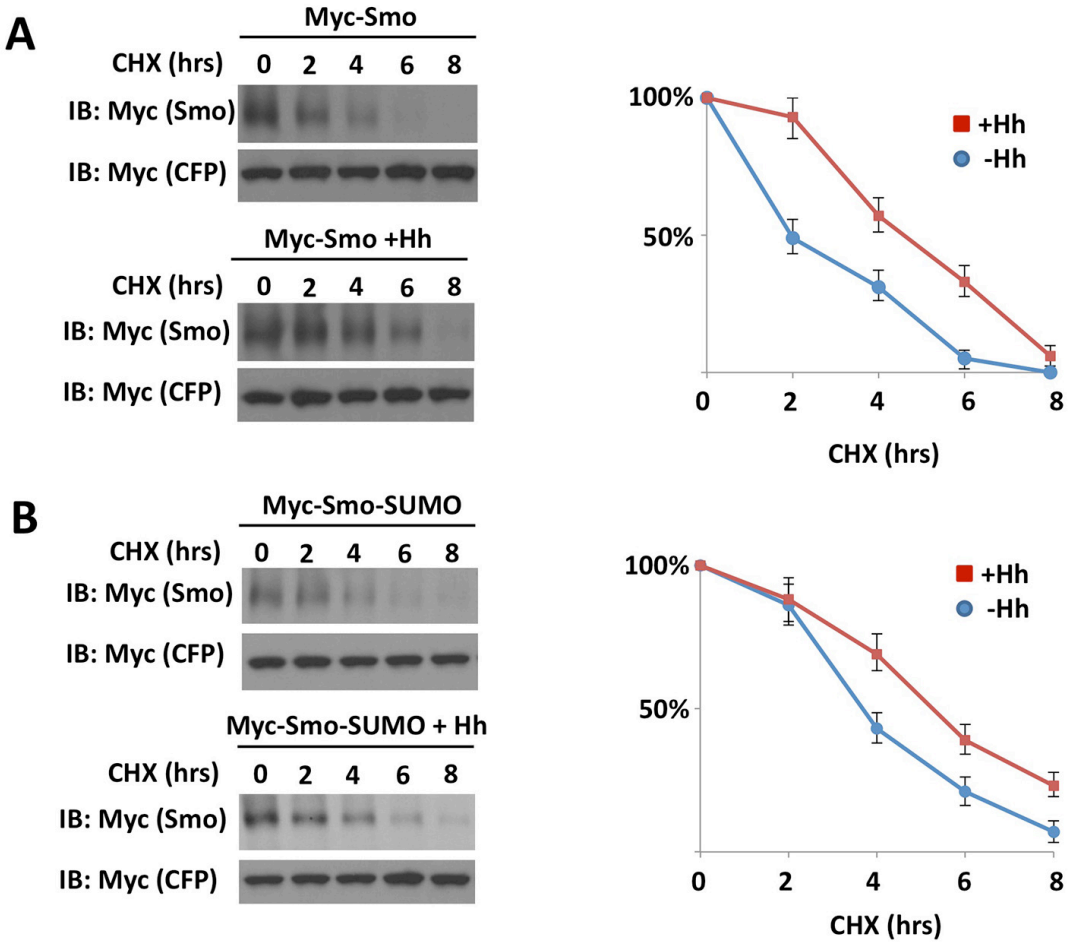

Figure S7 SUMO conjugation of Smo increase its stability–related to Figure 6

(A-B) S2 cells transfected with either Myc-Smo (A) or Myc-Smo-SUMO (B) in the presence or absence of Hh stimulation were treated with CHX for the indicated time periods, following by western blot analysis with Myc antibody. Myc-CFP was cotransfected as an internal control. Quantification of Myc-Smo levels at different time points was shown to the right. Data are mean ± SD from three independent experiments. Signal intensities at t=0 were defined as 100%. Of note, to ensure relatively equal level of Smo protein at t=0, more Myc-Smo DNA than that of Myc-Smo-SUMO was transfected and more DNA was transfected in the absence of Hh treatment compared with that treated with Hh-conditioned medium.